NASA-CR-205326

Development of a Composite Tailoring Technique for Airplane Wing

Progress Report/Renewal Proposal
Grant No. NAG2-908
Technical Monitor: Dr. Hiro Miura
NASA Ames Research Center

Principal Investigator: Aditi Chattopadhyay
Graduate Research Associate: Ratneshwar Jha
Department of Mechanical and Aerospace Engineering
Arizona State University
Tempe, Arizina 85287-6106

Objectives

- Composite wings have become increasingly popular in recent years due to significant potential of weight savings and stiffness tailoring. For aircraft wings made out of composite materials, aeroelastic tailoring presents an opportunity to enhance the aircraft performance by utilizing their unique stiffness and strength properties. Therefore, the goal of the current researh are as follows.

(1) Development of a new composite beam modeling technique to represent the principal load-carrying member in the wing. The theory includes the effect of through-the-thickness shear deformation which is important in laminated composites and is not included in the classical theory. A refined higher-order theory is used to describe the displacement field in each wall and appropriate boundary conditions are imposed to ensure the satisfaction of stress-free boundary conditions at the free surfaces. The theory is implemented using the finite element method.

(2) Development of a formal design optimization procedure to investigate the effect of composite tailoring on aeroelastic stability and structural characteristics of airplane wings. The composite structural analysis is coupled with unsteady aerodynamic analysis to solve the coupled aeroelastic equations of motion. The unsteady aerodynamic computations are performed using a panel code based on the Doublet Lattice Method and flutter/divergence speed is obtained using the V-g method. A hybrid optimization technique is implemented for the optimization to simultaneously include continuous and discrete design variables.

(3) Use the developd procedure to perform design optimization studies on realistic airplane configurations to investigate the various aeroelastic/structural/dynamic design issues.

Approach

Structural Analysis

The accurate and efficient prediction of structural response is very important for the investigation of aeroelastic tailoring using composite structures. The analysis of aircraft wings can be accomplished either through a detailed investigation of structural sections comprising spars, webs, ribs etc., or through the use of reduced structural models. The detailed analysis is computationally very expensive and is often impractical in design optimization and/or trade-off studies. Reduced structural models are more frequently used which include equivalent plate models and box beam models. Between these two, box beam models more closely represent real wing structures and more accurately account for elastic couplings.

A rectangular composite box beam model with taper and sweep is developed to represent the load carrying member of an aircraft wing (Fig.1). The single-celled composite box beam model is based on a higher-order composite laminate theory [10] and accounts for the distributions of shear strains through the thickness of each wall. The displacement field for each wall section is described by bending, warping and in-plane stretching.

For each of the individual plates, the higher-order displacement field is defined in local coordinate system as follows (Fig. 2).

$$
\begin{aligned}
u(x,y,z,t) &= u_0(x,y,t) + z\psi_x(x,y,t) \\
&\quad + z^2\xi_x(x,y,t) + z^3\zeta_x(x,y,t) \\
v(x,y,z,t) &= v_0(x,y,t) + z\psi_y(x,y,t) \\
&\quad + z^2\xi_y(x,y,t) + z^3\zeta_y(x,y,t) \\
w(x,y,t) &= w_0(x,y,t)
\end{aligned}
\tag{1}
$$

where u_0, v_0 and w_0 denote the displacements of a point (x, y) on the midplane and ψ_x and ψ_y are the rotations of the normal to the midplane about the y and x axes, respectively. The higher-order terms ξ_x , ζ_x, ξ_y and ζ_y represent beam warping in each plane. Making the assumption of small displacements and rotations, a linear strain-displacement relationship is used. The following constitutive relation is used for plates made of orthotropic materials.

$$
\begin{bmatrix} \sigma_1 \\ \sigma_2 \\ \sigma_3 \\ \sigma_4 \\ \sigma_5 \\ \sigma_6 \end{bmatrix} = \begin{bmatrix} Q_{11} & Q_{12} & Q_{13} & 0 & 0 & Q_{16} \\ Q_{12} & Q_{22} & Q_{23} & 0 & 0 & Q_{26} \\ Q_{13} & Q_{23} & Q_{33} & 0 & 0 & Q_{36} \\ 0 & 0 & 0 & Q_{44} & Q_{45} & 0 \\ 0 & 0 & 0 & Q_{45} & Q_{55} & 0 \\ Q_{16} & Q_{26} & Q_{36} & 0 & 0 & Q_{66} \end{bmatrix} \begin{bmatrix} \varepsilon_1 \\ \varepsilon_2 \\ \varepsilon_3 \\ \varepsilon_4 \\ \varepsilon_5 \\ \varepsilon_6 \end{bmatrix} \tag{2}
$$

The higher order terms are determined using the condition that the transverse shear stresses, σ_{xz} and σ_{yz}, vanish on the plate top and bottom surfaces. For composite plates made up of layers of orthotropic lamina, these conditions are equivalent to the requirement that the corresponding strains be zero on the surfaces. By making substitution for ψ_x and ψ_y in terms of ϕ_x and ϕ_y which are the shear angles at midplane about x and y axes respectively, the following refined higher-order displacement field is obtained.

$$u = u_0 - z\frac{\partial w_0}{\partial x} + z\left[1 - \frac{4}{3}\left(\frac{z}{h}\right)^2\right]\phi_x$$

$$v = v_0 - z\frac{\partial w_0}{\partial y} + z\left[1 - \frac{4}{3}\left(\frac{z}{h}\right)^2\right]\phi_y \qquad (3)$$

$$w = w_0$$

Based on the above displacement field, a four-node plate element is developed.

In the finite element formulation, the plate displacements at the mid-plane, u_0 , v_0 and w_0 are interpolated by Hermite cubic functions and the shear angles, ϕ_x and ϕ_y are interpolated using bilinear functions. For a higher-order plate element, there are 11 degrees of freedom at each node.

The governing equations of motion for an individual plate is derived using Hamilton's principle.

$$\int_{t_1}^{t_2} \delta\left[U - V + W_{nc}\right]dt = 0 \qquad (4)$$

where U, V and W denote the kinetic energy, the strain energy and the work done by external forces, respectively. Using the constitutive relations along with the strain-displacement relations, the element stiffness matrix K_e, the mass matrix M_e and the forcing vector F_e are derived from Eqn. 4 as follows.

$$K_e = \int_{V_e} B_e{}^T C_m B_e \, dV_e$$

$$M_e = \int_{V_e} \rho N_e{}^T N_e \, dV_e$$

$$F_e = \int_{A_e} N_e{}^T p(x, y, t) \, dA_e \qquad (5)$$

where V_e and A_e represent element volume and surface area, respectively and ρ denotes material density. The matrix C_m is material stiffness matrix and p is the air pressure. Matrices B_e and N_e relate the generalized coordinates to strains and displacements, respectively.

The construction of the box beam from plate elements is shown in Fig. 3. The quantities u, v, and w are displacements along x, y and z axis, respectively and θ_x, θ_y and θ_z are rotations along these directions. To make stiffness transformation possible, continuity of displacements and rotations are imposed at each of the four corners while the generalized forces

corresponding to higher order warping terms are set to zero. Through the use of coordinate transformation, the reduced stiffness matrix is expressed in the global form. Assembly of the element matrices leads to the following equation of motion for a general structural-aerodynamic system.

$$M\ddot{x} + C\dot{x} + Kx = Q_1 + Q_2 \tag{6}$$

where M, C and K denote global mass, damping and stiffness matrices respectively. The vector x represents structural elastic deformation. The quantities Q_1 and Q_2 denote aeroelastic forces and other forces due to gust, control surface motion etc. respectively

Aeroelastic Analysis

For aeroelastic stability analysis, the damping C and the non-aeroelastic forces Q_2 are ignored. Assuming simple harmonic motion, that is, $x = \bar{x}e^{i\omega t}$ and $Q_1 = \bar{Q}_1 e^{i\omega t}$ yields

$$(-\omega^2 M + K)\bar{x} = \bar{Q}_1 \tag{7}$$

$\bar{Q}_1$ can be expressed as a linear combination of $\bar{x}$ as follows.

$$\bar{Q}_1 = q_\infty F(i\omega)\bar{x} \tag{8}$$

where $F(i\omega)$ is the aerodynamic influence coefficient. Substituting for $\bar{Q}_1$ in Eqn (7) gives

$$(-\omega^2 M + K - q_\infty F(i\omega))\bar{x} = 0 \tag{9}$$

Equation 9 represents an eigen value problem and the solution of

$$\left|-\omega^2 M + K - q_\infty F(i\omega)\right| = 0 \tag{10}$$

provides the roots which determine the stability of the system. To solve the above problem, artificial damping is introduced and Eqn. 10 is rewritten as

$$\left|-\omega^2 M + (1+ig)K - q_\infty F(i\omega)\right| = 0 \tag{11}$$

The solution of Eqn. 11 yields the variations of g and ω with respect to q_∞. At the flutter point, the damping g=0.

The V-g method of flutter prediction is the classical method which is widely used. In this method, the aerodynamic forces need to be calculated for real ω only. However, the results are considered accurate only at the flutter point.

Hybrid Optimization

The inclusion of both continuous and discrete design variables significantly complicates the optimization problem. This is because the discrete design variables are not compatible with traditional gradient based optimization methods. Similarly, the continuous variable is not compatible with combinatorial optimization methods, such as branch and bound techniques, which require discrete values to operate. Therefore, a hybrid optimization technique developed by Chattopadhyay and Seeley which combines both types of design variables is used and is described next.

The general continuous/discrete optimization problem can be mathematically stated as follows.

Minimize $\quad f(\Phi_c, \Phi_d)$

Subject to $\quad g(\Phi_c, \Phi_d)_j \le 0 \quad$ where $\quad j = 1, 2, \ldots, \text{NCON}$

Side constraints $\quad \Phi_{c_l} \le \Phi_c \le \Phi_{c_u}$

$$\Phi_d \in [\Phi_{1_q}, \Phi_{2_q}, \Phi_{3_q}, \ldots, \Phi_{d_q}]$$

where f is the objective function, gj are the constraints, Φ_c are the continuous design variables and Φ_d are the discrete design variables which can be selected from among a set of q preselected values. The hybrid optimization procedure is based on Simulated Annealing (SA) where the design space is sampled by repeatedly perturbing the discrete design variables. At each iteration of the SA procedure, the objective function is minimized with respect to the continuous variables using a BFGS search algorithm. This significantly improves the efficiency of the hybrid algorithm by directing the search using the gradient information when available. The constrained problem is formulated using a penalty function approach.

Results

The development of the higher order box-beam model has been completed. Comparisons of the results have been made with experimental data (Chopra et al.), results from a quasi-analytical method (Chopra et al.), and the variational asymptotical approach (VABS, Hodges et al.). The

dimensions of the test beams are defined in Fig. 4. Beams with various ply lay-ups have been evaluated, of which only symmetric lay-up results are presented here (Figs. 5 and 6). The ply angles for the top and bottom walls are 45° and those for the side walls are 45°/-45°. This kind of lay-up exhibits bending-torsional coupling, hence a bending load also generates beam twist. For the bending induced twist, results from the present model are closest to the test data. Good correlations are also observed with experiments for the bending slope. Further results can be found in Ref. 1.

A simple optimization problem has been formulated to study the effects of aeroelastic tailoring. A standard elliptic static aerodynamic load distribution has been assumed. The objective is to minimize the weight of the box beam which represents the structural member of an airplane wing. Constraints are placed on the flutter speed and the maximum allowable stresses. The flutter/divergence speed (V_f) is constrained to be greater than 450 knots equivalent air speed (KEAS) at a flight condition of Mach 0.7 at sea level. The Tsai-Wu failure criterion is imposed on the critical ply stresses at the root section where material failure is most likely to occur.

Results obtained using the hybrid optimization procedure are presented in Tables 1 and 2 and in Figs. 7-10. Optimization results are compared with a reference design, which is selected based on engineering judgment. It should be noted that the optimum design is independent of the initial design due to probabilistic nature of the hybrid optimization procedure. The penalty function value is presented in Fig.7 at each iteration of the simulated annealing algorithm which consists of several BFGS evaluations. Both the trial designs and the best state so far are presented. Initially, the flutter constraint is violated which results in very large values of the penalty function which are not presented due to the scale of the graph. The optimum state is reached in less than 100 iterations and the optimization procedure is terminated after 250 iterations since no better design could be found.

There is a significant reduction in the weight of the structural member of the wing (32%, Fig.8) along with a large improvement in the flutter speed (75%, Fig.9) due to the optimization. The Tsai-Wu stress criterion is satisfied by the reference as well as the optimal design (Fig. 10). Since the wing root chord for the reference and the optimal wings are nearly same (Table 2), weight reduction is due to the smaller number of plies for the optimal wing. Through optimization of the stacking sequence, even a lower wall thickness provides higher flutter speed.

Study of the frequencies and modes for flutter show important trends. For the reference wing, the second mode, which is a coupled bending and lag mode with a natural frequency of 34 Hz, flutters at 29 Hz. The first torsion mode is the sixth mode with a natural frequency of 164 Hz.

At the flutter condition, the frequencies of the second and the sixth modes almost coalesce and the sixth mode also flutters at a slightly higher speed. For the optimal wing, flutter occurs for the fifth mode (at 74 Hz), which is the first torsion mode with the natural frequency of 160 Hz. The first four modes are bending or coupled bending/lag modes. Thus the optimization essentially stiffens the bending modes to increase the flutter speed.

Since the aspect ratio and taper ratio are fixed for this study, smaller root chord also means smaller span and lower wing area. The optimal value of the wing root chord is very near to the minimum value specified to have high stiffness. This trend is expected in the absence of other design considerations such as wing loading (which affects landing/take-off speed, maneuverability etc.) and internal fuel volume.

Future Work

The V-g method of flutter prediction is only valid at the flutter point. Therefore, the s-domain method of flutter analysis, which provides both pre- and post-flutter history, will be adopted and will be integrated with the composite structural analysis procedure. Further details of the s-domain method is given in Annexure 1. The developed analysis procedure will then be used within the design optimization loop to provide aeroelastically tailored wing designs.

Publications

1. Chattopadhyay, A., Zhang, S. and Jha, R., "Stuctural and Aeroelastic Analysis of Composite Wing Box Sections Using Higher-Order Laminate Analysis," 37th AIAA/ASME/ASCE/AHS/ASC Structures, Strucurat Dynamics and Materials Conference, Salt Lake City, Utah, April 15-17, 1996. (Submitted to "The International Journal of Computers and Mathematics" for publication)

2. Chattopadhyay, A. and Jha, R., "Application of Hybrid Optimization Technique for Improved Aeroelastic Performance of Composite Wings," 6th AIAA/NASA/USAF Multidisciplinary Analysis and Optimization Symposium, September 4-6, 1996/Bellevue, WA.

Table 1 Wing Parameters.

	Reference	Optimum
Number of plies	28	18
Root chord (in.)	15.0	15.4
Wall thickness (in)	0.14	0.09
Stacking Sequence		
top and bottom walls	$[0°/90°]_{14}$	$[0°/-45°]_{9}$
side walls	$[45°/-45°]_{14}$	$[0°/0°]_{9}$

Table 2. Frequencies and Modes

Mode Number	Reference		Optimum	
	Mode	Freq. (Hz)	Mode	Freq. (Hz)
1	B	9.4	B	8.75
2	L, B	34.1	L, B	34.7
3	B, L	50.7	B, L	46.8
4	B, L	116.9	B	107.7
5	L	154.7	T	159.5
6	T	163.6	L, B	170.1
Flutter Point	2nd mode, 29 Hz		5th mode, 74 Hz	

Legend: B - Bending L - Lag T - Torsion

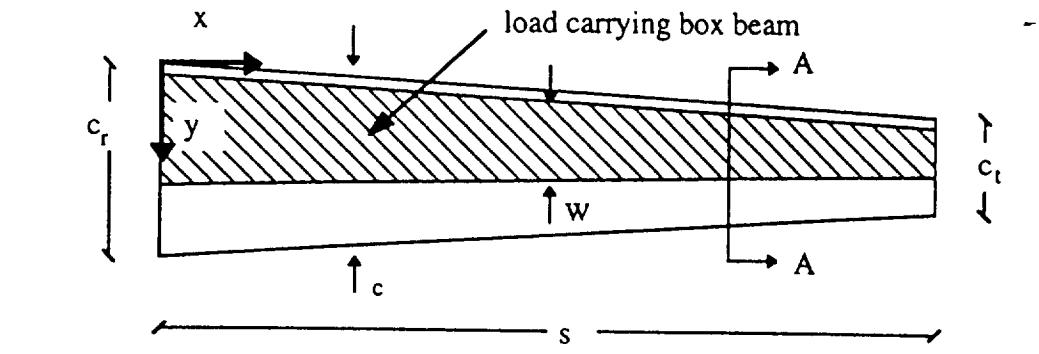

(a)

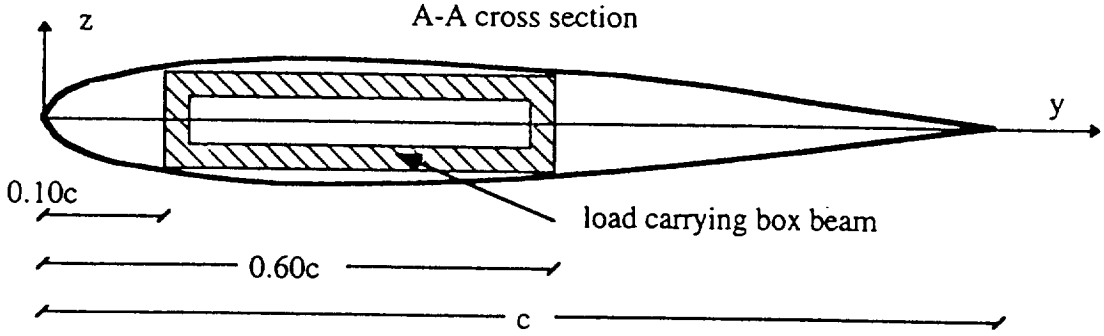

(b)

Figure 1. Wing Geometry (a) top view (b) side view

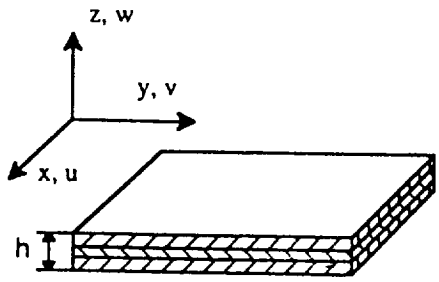

Figure 2. Plate model

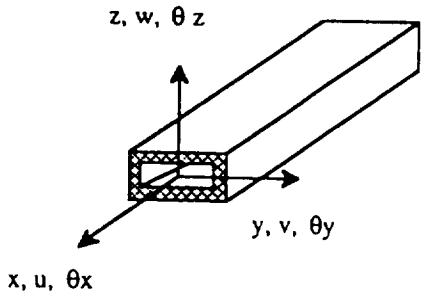

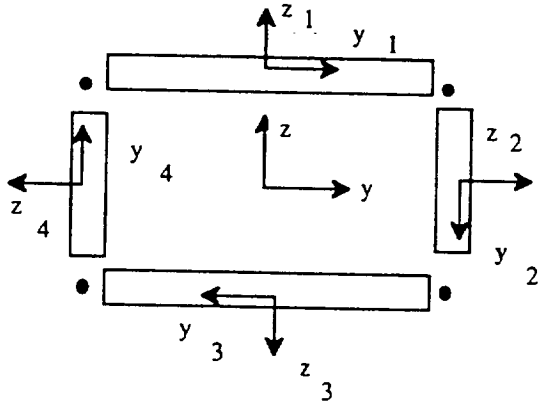

Figure 3. Beam construction

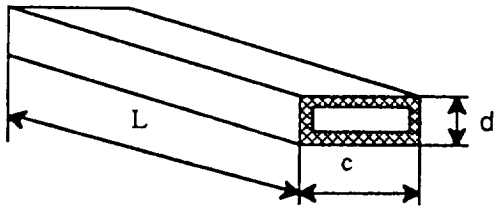

	L/d=56	L/d=29
L (in)	30	30
d (in)	0.537	1.025
c (in)	0.953	2.060
Ply thickness (in)	0.005	0.005
Wall thickness (in)	0.03	0.03

Figure 4. Test beam dimensions

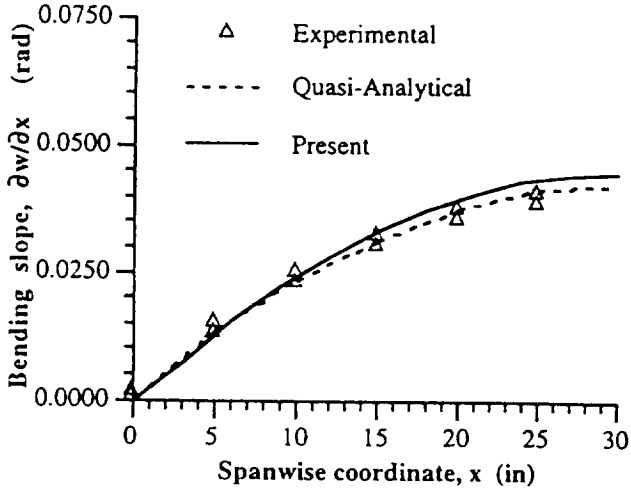

Fig. 5 Bending slope of $[45°]_6$ thin-walled beam under 1 lb.bending load at tip

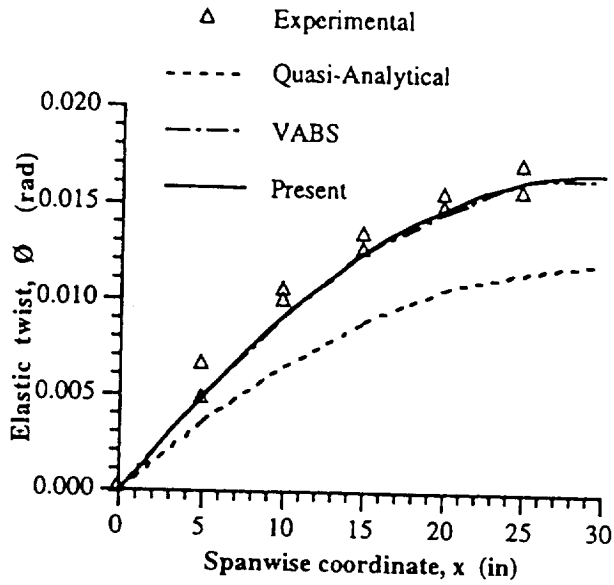

Fig. 6 Bending-induced twist of [45°]6 thin-walled beam under1 lb. bending load at tip

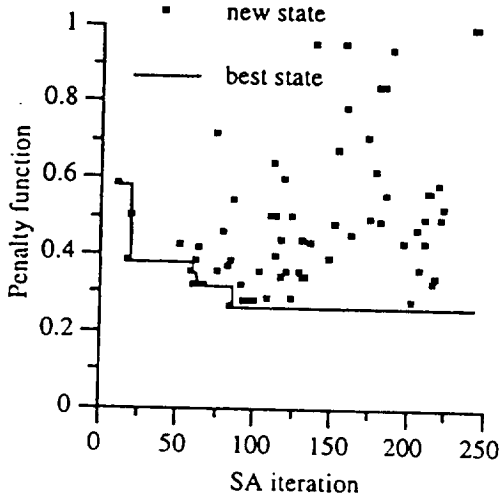

Fig 7 Penalty function iteration history

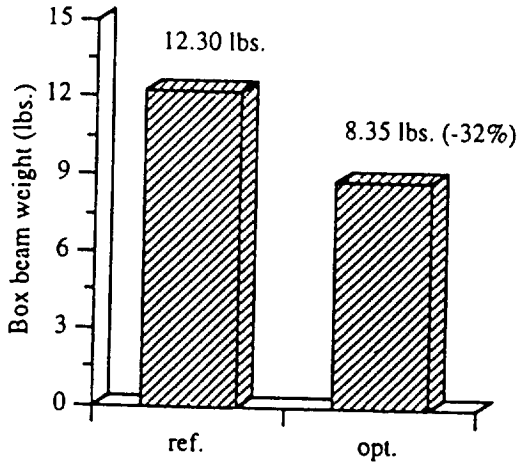

Fig.8 Box beam weight.

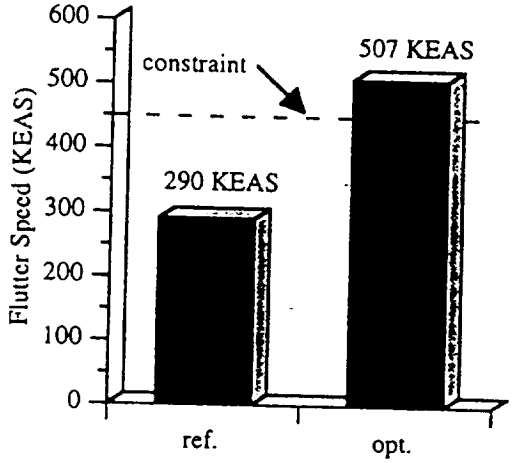

Fig. 9 Flutter Speed.

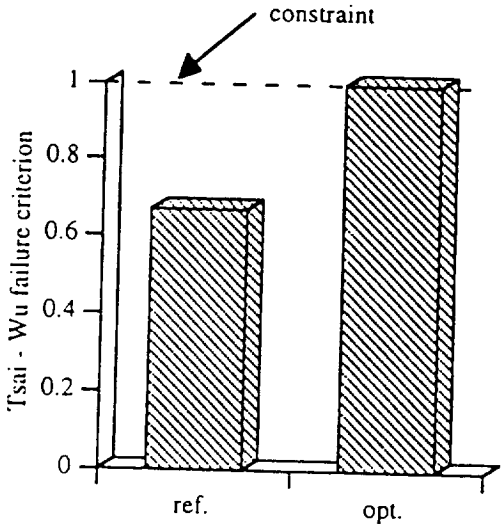

Fig 10 Tsai - Wu failure criterion.

Annexure 1

Flutter Analysis using the s-domain method

Equation of motion for a general structural-aerodynamic system is given as

$$M\ddot{X} + C\dot{X} + KX = Q1 + Q2 \tag{1}$$

where M, C and K represent mass, damping and stiffness matrices respectively. Q1 and Q2 denote aeroelastic forces and other forces due to gust, control surface motion etc. For aeroelastic stability analysis, damping C and non-aeroelastic forces Q2 are ignored. Laplace transform of the resulting equation yields

$$(s^2M + K)\overline{X} = Q1(s) \tag{2}$$

Q1(s) can be expressed as a linear combination of $\overline{X}$ as

$$Q1(s) = q_\infty F(s)\overline{X} \tag{3}$$

where F(s) can be regarded as the aerodynamic transfer function. Substituting for Q1(s) in Equation (2) gives

$$(s^2M + K - q_\infty F(s))\overline{X} = 0 \tag{4}$$

This is an eigen value problem and the solution of

$$\left|s^2M + K - q_\infty F(s)\right| = 0 \tag{5}$$

gives the roots which determine the stability of the system. For stability, all real roots should be negative. At flutter condition, one of the roots is purely imaginary. The main difficulty in solving equation (5) arises in obtaining the aerodynamic transfer function F(s). It is assumed that F(s) equals F(iw), where w is a real value (as for the V-g method). F(iw) is obtained from the Doublet Lattice Method code mentioned earlier.

F(s) is expressed in Padè Approximant form

$$F(s) = a + bs + cs^2 + \sum \frac{\alpha s}{\beta s + r} \tag{6}$$

and the coefficients are evaluated using a least square fit. Then equation (5) is solved in complex s-domain to obtain the roots of the system. As mentioned earlier, the solution (frequency and damping) is valid at all speeds, not just the flutter speed, unlike the V-g method. This method is also advantageous in active control of aeroelastic systems.